Influence of side chain linker length on ion-transport properties of polymeric ionic liquids

Jordan R. Keith, Santosh Mogurampelly, Bill K. Wheatle, Venkat Ganesan

Department of Chemical Engineering, University of Texas at Austin, Austin, Texas 78712, USA

ABSTRACT: We used atomistic molecular dynamics simulations to study the properties of polymerized 1-*alkene*-3-butylimidazolium-hexafluorophosphate, a polymerized ionic liquid electrolyte, and characterized the influence of the linear alkene length on the mobility of the hexafluorophosphate ions. Consistent with experimental observations, our simulations indicate that as the alkene length increases, the diffusivity of hexafluorophosphate anion monotonically increases. We demonstrate that such a trend arises from the influence of linker segments on the intermolecular ion hopping rates, which is in turn modulated by intermolecular cationic separation distances.

Keywords: Polymeric Ionic Liquid, Diffusion, Hopping

Lithium-ion batteries continue to be a popular thrust of research for portable power storage and energy solutions.[1–3] A particular focus of the efforts in this context has been on the design of polymer materials which can simultaneously provide the mechanical strength and charge transport properties desired in electrolytes for such applications.[4–7] However, liquid and neutral-polymer electrolyte materials consisting of simultaneously mobile anions and cations exhibit performance-hampering charge polarization as a result of the coordinated diffusion of counterions and subsequent buildup of anions near the anode.[8–10] In such a context, single-ion conductors (SICs), representing materials in which either the anions or cations are covalently attached to a macromolecule of low mobility, have been proposed as a solution. In such materials, the coordinated diffusion of the ion pairs is significantly reduced, and as a result, the charge polarization effects are virtually eliminated, resulting in transference numbers close to unity.[11–15]

Ionic liquids (ILs) are a class of materials which have attracted significant attention in view of their excellent chemical stability, low volatility and toxicity, and desirable compatibility with various polar and ionic media.[16–18] Due to such features, polymerized ionic liquids (polyILs) have emerged as popular SIC materials. Such efforts were pioneered by Ohno and Ito's work on polymerizing imidazolium and sulfonamide salts.[19] Subsequent work by Ohno demonstrated that improvements could be made on the conductivity by swapping the anionic and cationic moieties, and by doping the polyILs with salts containing plasticizing ions.[20] Comprehensive reviews have summarized the progress made since then for polyILs as polyelectrolyte materials for batteries and other applications,[21,22] and we refer the interested reader to such sources for a discussion of the accompanying developments.

A number of different physicochemical parameters have been examined to understand (and optimize) the transport properties of polyILs.[23–25] The motivation for the present study comes from a set of (superficially) conflicting experimental reports pertaining to the influence of the length of the side chain of ILs upon the transport properties of polyILs. Specifically, for polymerized 1-vinyl-3-*alkyl*imidazolium, Salas-de la Cruz and coworkers reported a decrease in conductivity with increasing length of the Group 1 alkyl side chain in Figure 1.[26] In contrast, Choi and coworkers reported increasing ionic conductivity with increasing Group 2 alkyl length (Figure 1) for a similar imidazolium-based polyIL.[27,28] Together, such observa-

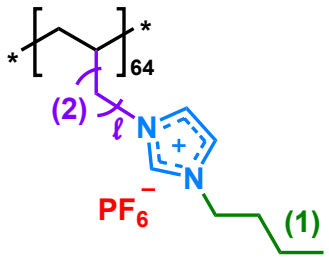

Figure 1: Schematic of polymer used in this study. Groups are color-coded and alkyl segments are numbered for reference in body text. *Terminated on left with H and right with CH_3

tions have raised the question,[29] "what are the mechanisms underlying the influence of the linker side-chain length on the transport properties of polyILs?"

In the present communication, we report the results of atomistic computer simulations which were used to study the structure and mechanisms underlying the effect of Group-2-linker length (l) on the transport of non-polymerized ions (Figure 1). We quantify the structural organization in such systems through the radial distributions and the average intermolecular separation between cationic groups. Inspired by our recent findings in the context of ion transport mechanisms in polyILs,[30] we employ an analysis tool for identifying ionic association/dissociation processes to elucidate the connection between the interchain ion-hopping mechanism and the PF_6^- diffusion, and thereby identify the origins underlying the influence of side chain linker length.

In a recent article, we studied the transport properties of PF_6^- counterions in poly(1-butyl-3-vinylimidazolium) electrolyte membranes (which corresponds to the case of $l = 0$ in our notation of Figure 1).[30] In such a context, we employed the force field parameters originating from Jorgensen's optimized potentials for liquid simulations-all atom (OPLS-AA) force field,[31] modified by Sambasivarao et. al.[32] for use in ionic liquids. Additionally, Mogurampelly et. al. developed intramolecular parameters for the bond, angle, and dihedral interactions of the polyethylene backbone.[30] We adopted those parameters in the present study, while incorporating additional parameters for the linker atoms. Tables S1-S7 of the Supporting Information provide a complete list of these parameters, and section I.B describes the development of the force field parameters in additional detail. Quantum chemistry calculations were employed to obtain the charge distribution for the monomers. The software

package Gaussian 09 was used to optimize the monomers and to map the electrostatic potential using the B3LYP functional with the 6-311G(d,p) basis set.[33] The antechamber tool was used to collect the partial charge of each atom.[34,35]

Atomistic simulations were carried out using LAMMPS software.[36] The polymers were constructed and packed randomly into a simulation box containing eight polyILs of 64 monomers each, along with 512 PF_6^- counterions.[37] Simulations in the present work evaluate Coulombic interactions for particles within 10 Å using a direct sum, and using the particle-particle particle-mesh solver with a tolerance of 1×10^{-5} outside of that cutoff.[38,39] Lennard-Jones intermolecular interactions were evaluated with the same cutoff, while employing tail corrections. Simulations in the present work were conducted in the NPT ensemble, adjusting temperature every 0.1 ps and pressure every 1 ps using a Nosé-Hoover thermostat and Parrinello-Rahman barostat, with periodic boundary conditions and fixed linear momentum.[40–43] All simulations were conducted with a timestep of 1 fs. Section I.D of the Supporting Information details the above simulation procedure, along with a complete description of the initialization and equilibration procedures.

We begin our discussion of results by presenting the focal result of this article; namely, the diffusivity of PF_6^- ions as a function of linker size (2(a)) and temperature (Figure 2(b)). The mean squared displacement (MSD) of such PF_6^- ions were used to determine their diffusivity through the Einstein relation:

$$D = \lim_{t\to\infty} \frac{1}{6t} \left\langle \left(\mathbf{r}(t) - \mathbf{r}(0)\right)^2 \right\rangle, \tag{1}$$

where $\mathbf{r}(t)$ denotes the position of PF_6^- ions at time t. The results for the mean-squared displacements of the ions and the slopes of a power law fit to such results are presented in section II.A of the Supporting Information. From the results displayed in Figure 2(a) at a specified temperature, diffusivity is seen to increase as the linker length increases, matching the experimental results of Choi and coworkers.[27,28]

Structural characteristics such as aggregate sizes and scattering profile have been widely used in prior studies to understand the mechanisms underlying transport phenomena in polymer electrolyte and SIC systems.[15,46–51,51,52] Figure 3 displays the radial distribution

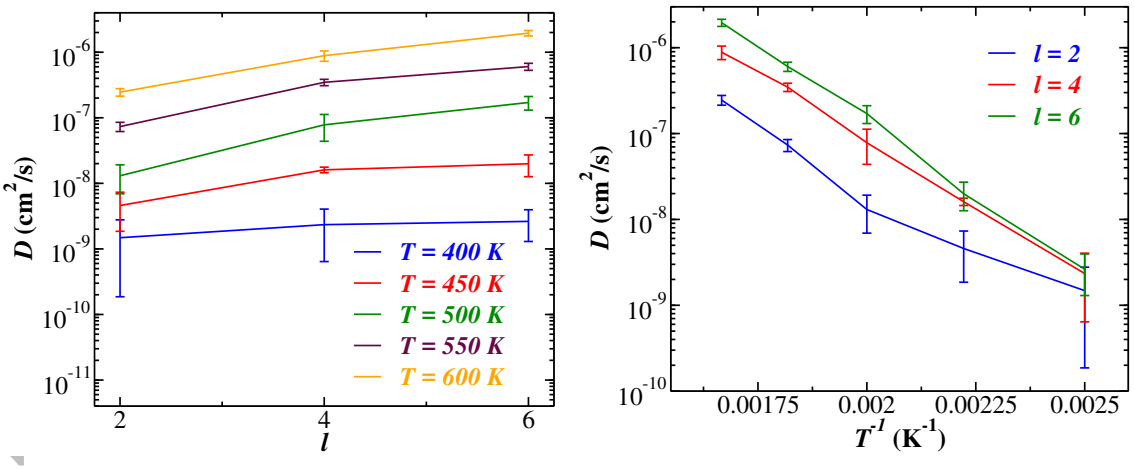

Figure 2: (a) Diffusivity as a function of linker length l (b) Diffusivity as a function of inverse temperature for polyILs of different linker sizes l. The lines represent a guide to the eye.

functions, $g(r)$, for the anion-cation pairs for the systems considered in the present article. Specifically, the cation is represented by the center of mass of imidazolium-ring atoms owing to the dominant share of positive charge, while the anion is represented by its full center of mass. The strongest electrostatic interactions exist between PF_6^- and these atoms, justifying their incorporation into the cationic center of mass. A sharp and consistent peak is seen for all linker sizes at an interionic distance of 5.5 Å. This suggests that the cation-anion local structure (with respect to the distance characterizing the first peak) is not influenced by the size of the linker groups in the polyIL. However, the most notable difference can be found in the intensity of the first peak, which is seen to increase monotonically with the size of the linker. Such trends are indicative of a stronger interaction between the cation and anion for larger linker sizes, and can be understood to be a result of the weaker impact of backbone related constraints hindering the ion pair coordinations.

A second peak is seen in $g(r)$ at a distance of 12.5 Å for $l = 4$ and 6, but is seen to be shifted to 11-11.5 Å for $l = 2$. Such trends are consistent with our results for $l = 0$ reported in Mogurampelly et al.,[30] wherein it was shown that relative to pure (non-polymerized) IL, the polymerization of the IL leads to a closer cation-anion second peak. It may be envisioned that systems with longer linker chains exhibit a behavior closer to non-polymerized ILs due to the accompanying reduction in backbone-related constraints. The extent of sec-

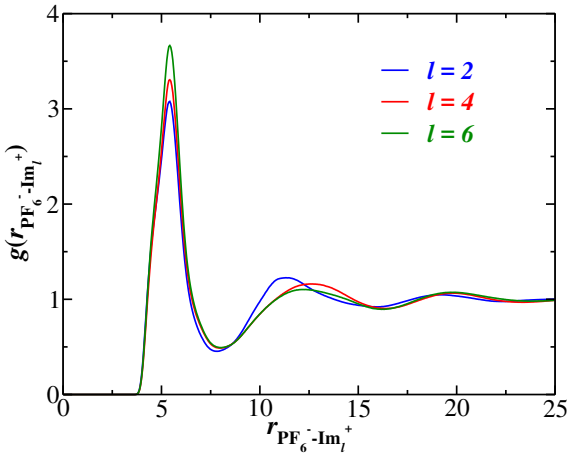

Figure 3: Radial distribution function of cation-anion coordination at 500 K.

ond coordination shell and corresponding peak value may indicate slightly increased ionic displacements with linker length. However, since the first peak is stronger, it is not clear whether the combined structural features revealed by $g(r)$ could explain the effect of linker length on ionic diffusivities. Overall, the above results indicate that, at the level of equilibrium cation-anion coordination behaviors, there are no *specific signatures* which rationalize the enhanced PF_6^- diffusivities observed for longer linker systems.

In a recent work from our group,[30] we used atomistic-molecular-dynamics simulations to demonstrate that ion transport in polyILs occur through a mechanism involving intra- and inter-molecular ion hopping through the formation and breaking of ion-associations. As a consequence, the ion mobilities in polyILs were shown to be inversely correlated to the average lifetimes of the cation-anion associations. Such results were shown to be in contrast with the behavior in pure ILs, wherein the structural relaxation times served as the critical parameter underlying ion mobilities.[30,53,54] Motivated by such earlier findings, in the present work, we sought to characterize whether the linker-size-dependent ion diffusivities are correlated to the respective average lifetimes of the ion associations, and if so, the manner by which the linker size influences the latter time scales.

In the context of polyILs, we previously showed that the continuous time autocorrelation function (defined below) and the associated time scales were the relevant quantities which tracked the ion diffusivities.[30] Such a correlation function was proposed by Chandra,[55] and invokes an "association" variable $h(t)$, which has a value of unity when a pair of ions is

within a cutoff distance (chosen as 6.5 Å in our work based on the coordination behavior between the ions), and is null otherwise.[30] Based on the association variable, we define a function $H(\tau)$ to hold a value of unity as long as that pair of ions remains associated. Once dissociated, $H(\tau)$ is assigned a value of zero, irrespective of the ion-association state in the future frame:

$$H(\tau) = \begin{cases} 1, & \Big(r \leq 6.5\text{Å}\Big) \wedge \Big(h(t) = 1\Big) \forall \Big(t_0 \leq t < t_0 + \tau\Big) \\ 0, & \text{otherwise.} \end{cases} \tag{2}$$

In a physical sense, the variable $h(t)$ simply represents the association between two ions at time t. The function $H(\tau)$ represents the continuous association of two ions from time t_0 to $t_0 + \tau$ and its characteristic time scale is the average lifetime of ion associations. To quantify the time scales of ion-pair associations, we define the time correlation function $S(\tau)$:[55]

$$S(\tau) = \frac{\big\langle h(t_0) H(t_0 + \tau) \big\rangle}{\big\langle h \big\rangle}. \tag{3}$$

The time correlation function $S(\tau)$ can either be numerically integrated, or alternatively, fit to a stretched exponential function and analytically integrated to obtain the average lifetime of ion associations, τ_S,[56]

$$S(\tau) = a_0 \exp\left(- \Big(\frac{\tau}{a_1}\Big)^{a_2} \right) \tag{4}$$

and

$$\tau_S = a_0 a_1 \Gamma\left(1 + \frac{1}{a_2}\right). \tag{5}$$

In Figure 4(a), we present results for the ion diffusivities as a function of τ_S obtained from fitting the decay to the stretched exponential function. We observe that the ion diffusivities in different polyIL linker systems can indeed be collapsed onto an approximately universal function when plotted in such a representation. Such results are consistent with the conclusions of our previous work,[30] and suggest that the mechanisms underlying the results displayed in Figure 2(b) are likely tied to the influence of the linker on the average lifetimes of the ion-pairs. Such a reasoning is confirmed in the results of Figure 4(b), which

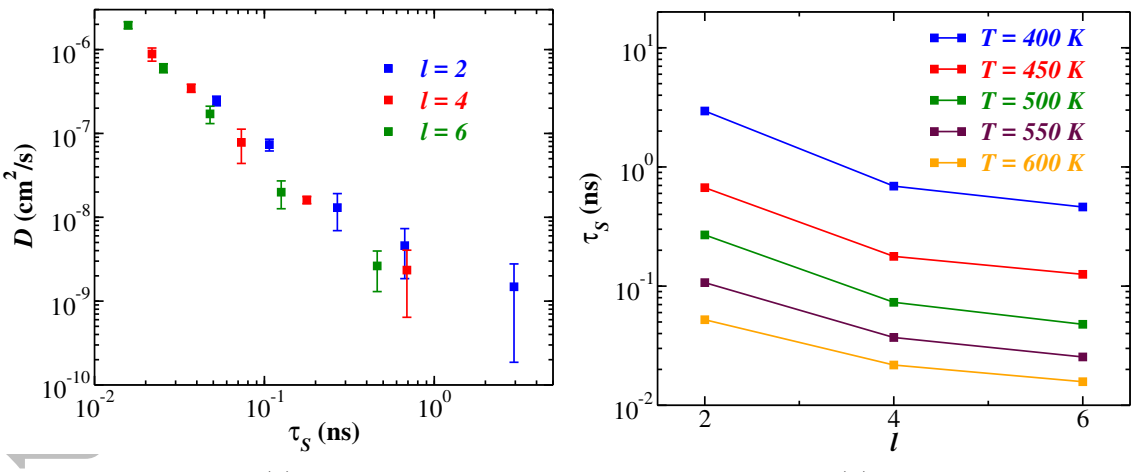

(a) (b)

Figure 4: (a)Diffusivity of PF_6^- as a function of τ_S for different linker lengths l and temperature T; and (b) Average lifetime of ion pairs, τ_S, as a function of linker length l and temperature T. The lines represent a guide to the eye.

explicitly displays the average lifetimes of the ion-pairs τ_S as a function of the linker length and temperature. Therein, it can be seen that with increasing linker length, there is a reduction in average lifetimes of the ion-associations τ_S — a result which mirrors the behavior observed for the ion diffusivities (Figure 2(a)).

Since the ion pair lifetimes are expected to be influenced by the number and rate of inter/intramolecular hopping events, we turn our attention to the latter characteristics and the influence of linker size upon such features.[30] For such an objective, we use a 1 ps time interval to collect the association variable $h(t)$, which changes from null to unity (or unity to null) when the PF_6^- ion becomes associated (dissociated) with a cation. We identified two categories of hopping events: intramolecular and intermolecular. Intramolecular hopping events characterize hopping motion of a PF_6^- ion from monomer to monomer on the same polymer. In contrast, intermolecular hopping events represent PF_6^- hopping among monomers of different polymers. Section II.D of the Supporting Information describes hopping events in detail, supplying exact definitions and special examples to ensure the reader's understanding.

In Figure 5 we present results depicting the number of intra- (denoted as N_1) and intermolecular (N_2) hopping events as a function of the linker length and temperature. We observe that polyILs possessing longer linker segments exhibit a larger number of intermolec-

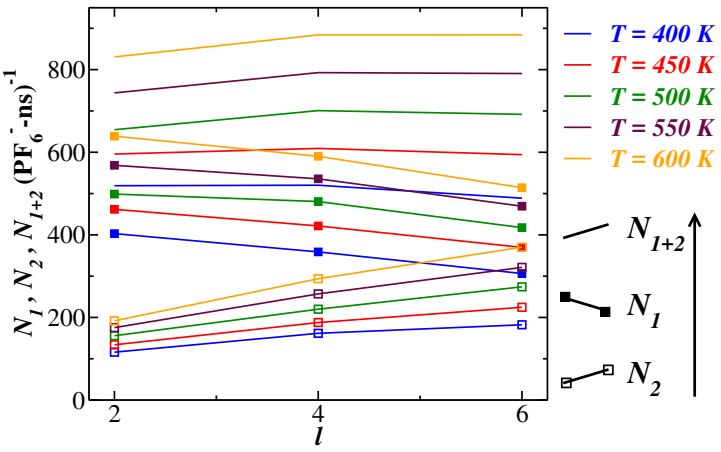

Figure 5: Frequency of intra (solid symbols, N_1), inter (open symbols, N_2) and total (no symbols) molecular hopping events per PF_6^- per ns. Lines represent a guide to the eye.

ular hopping events, N_2, and a smaller number of intramolecular events, N_1. Moreover, it can be seen that the total number of hopping events ($N_1 + N_2$) increases with increasing linker size. Together, the results indicate that the transition to longer linkers leads to a larger number of intermolecular-ion-hopping events, which lowers the average lifetimes of the ion associations and leads to higher ion mobilities.

As a final step in the understanding of the ion mobility characteristics, we seek to identify the origin of the linker size's influence on the intermolecular hopping events. In this regard, we were inspired by the works of Annapureddy[57] and Salas-de la Cruz,[26] which pointed to the intermolecular separation distance of polymerized-ionic groups as an important length scale in ionic liquids.[26] To characterize such a measure, we compiled the average intermolecular-nearest-neighbor distance between cationic centers-of-mass, d_p. The results are presented in Figure 6, wherein it can be seen that an increase in the linker size leads to a reduction in the intermolecular distance between cationic Im^+ groups, d_p.

The above results indicate that the influence of linker size on the intermolecular hopping events can be traced back to the role of the linkers in modulating d_p. More explicitly, an increase in the linker size of polyILs leads to more proximally located intermolecular cationic groups, which increases the frequency of intermolecular hopping events and the associated rate of ion pair hopping events. Such characteristics manifest macroscopically as enhanced PF_6^- mobilities (and conductivities).

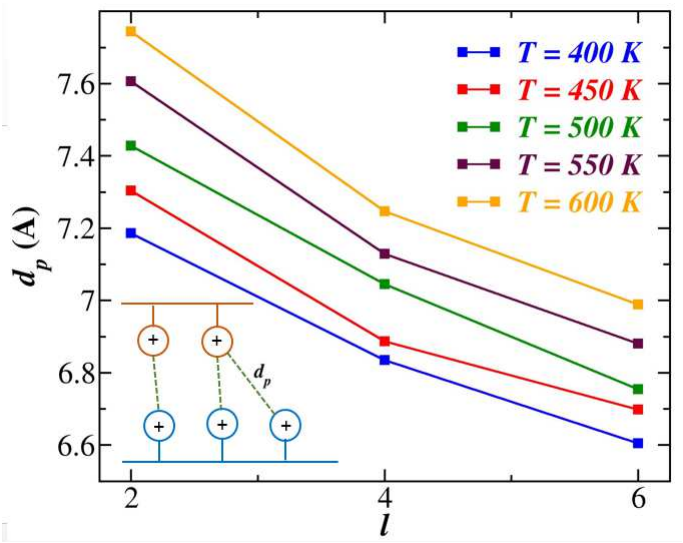

Figure 6: Average minimum intermolecular distance d_p between Im^+ as a function of the linker size l and temperature. The lines represent a guide to the eye.

We propose that our above finding is consistent with the (apparently) conflicting experimental observations of Salas-de la Cruz et al., who reported a decrease in conductivity with increasing length of the Group 1 alkyl side chain in Figure 1.[26] Our results showed a closer approach of cationic groups due to the increased length and flexibility of the Group-2 linker segment. In contrast, extending the Group 1 alkyl chain, such as in the work of Salas-de la Cruz, is more likely to reduce the possibilities for cation rearrangement and increase the corresponding intercationic distances. Therefore, for situations where the Group-1 side chain length is increased, we expect the propensity for intermolecular hopping to be lowered, and the corresponding rates of ion pair hopping events to become slower. In turn, such characteristics are expected to manifest in lower ion mobilities as noted in the experiments.[26]

In summary, this study probed the effects and mechanisms underlying changes in monomer linker length on the transport properties of polyILs using atomistic simulations. Our simulation results were consistent with experimental observations that an increase in the linker length leads to a corresponding enhancement in anion mobilities. We rationalized our results and related experimental observations by demonstrating that ion motion in such systems proceeds primarily through intra- and intermolecular hopping. Moreover, an increase in the linker length was shown to increase the propensity for intermolecular ion hopping through the influence of the former upon the intermolecular cationic distances. The results of our

study highlight the intermolecular cationic distances as a novel physicochemical parameter, which can be tuned to influence the ion transport characteristics of polymerized ionic liquid membranes.

ACKNOWLEDGMENTS

The authors acknowledge the Texas Advanced Computing Center (TACC) at The University of Texas at Austin for providing computing resources that have contributed to the research results reported within this paper. We acknowledge funding in part by grants from the Robert A. Welch Foundation (Grant F1599), the National Science Foundation (DMR-1306844), and the Donors of the American Chemical Society Petroleum Research Fund (56715-ND9).

References

1. J. Tarascon, Nature **414**, 359 (2001).
2. J. Song, Y. Wang, and C. Wan, Journal of Power Sources **77**, 183 (1999).
3. M. Marcinek, J. Syzdek, M. Marczewski, M. Piszcz, L. Niedzicki, M. Kalita, A. Plewa-Marczewska, A. Bitner, P. Wieczorek, T. Trzeciak, et al., Solid State Ionics **276**, 107 (2015).
4. M. Watanabe, Y. Suzuki, and A. Nishimoto, Electrochimica Acta **45**, 1187 (2000).
5. Y. Lin, J. Li, Y. Lai, C. Yuan, Y. Cheng, and J. Liu, RSC Advances **3**, 10722 (2013).
6. R. C. Agrawal and G. P. Pandey, Journal of Physics D: Applied Physics **41**, 223001 (2008).
7. A. M. Christie, S. J. Lilley, E. Staunton, Y. Andreev, and P. G. Bruce, Nature **433**, 50 (2005).
8. G. Jaffe? and J. A. Rider, ‘ **20**, 1071 (1952).
9. J. R. Macdonald, Physical Review **92**, 4 (1953).

0. J. R. Macdonald, The Journal of Chemical Physics **61**, 3977 (1974).

1. R. J. Klein, S. Zhang, S. Dou, B. H. Jones, R. H. Colby, and J. Runt, Journal of Chemical Physics **124**, 144903 (2006).

2. K.-J. Lin, K. Li, and J. K. Maranas, RSC Advances **3**, 1564 (2013).

3. X. G. Sun, C. L. Reeder, and J. B. Kerr, Macromolecules **37**, 2219 (2004).

4. H. Markusson, H. Tokuda, M. Watanabe, P. Johansson, and P. Jacobsson, Polymer **45**, 9057 (2004).

5. K. Lu, J. F. Rudzinski, W. G. Noid, S. T. Milner, and J. K. Maranas, Soft Matter **10**, 978 (2014).

6. M. Armand, F. Endres, D. R. MacFarlane, H. Ohno, and B. Scrosati, Nature Materials **8**, 621 (2009).

7. P. J. Griffin, Y. Wang, A. P. Holt, A. P. Sokolov, P. J. Griffin, Y. Wang, A. P. Holt, and A. P. Sokolov, Journal of Chemical Physics **144**, 151104 (2016).

8. H. Ohno, Bulletin of the Chemical Society of Japan **79**, 1665 (2006).

9. H. Ohno and K. Ito, Chemistry Letters **27**, 751 (1998).

0. H. Ohno, Electrochimica Acta **46**, 1407 (2001).

1. O. Green, S. Grubjesic, S. Lee, and M. A. Firestone, Journal of Macromolecular Science R , Part C: Polymer Reviews **49**, 339 (2009).

2. D. Mecerreyes, Progress in Polymer Science (Oxford) **36**, 1629 (2011).

3. K.-J. Lin and J. K. Maranas, Physical chemistry chemical physics : PCCP **15**, 16143 (2013).

4. Y. Ye and Y. A. Elabd, Polymer **52**, 1309 (2011).

5. M. Lee, U. H. Choi, R. H. Colby, and H. W. Gibson, Chemistry of Materials **22**, 5814 (2010).

6. D. Salas-de-la Cruz, M. D. Green, Y. Ye, Y. A. Elabd, T. E. Long, and K. I. Winey, Journal of Polymer Science Part B: Polymer Physics **50**, 338 (2012).

7. U. H. Choi, A. Mittal, T. L. Price, M. Lee, H. W. Gibson, J. Runt, and R. H. Colby, Electrochimica Acta **175**, 55 (2015).

8. U. H. Choi, Y. Ye, D. Salas De La Cruz, W. Liu, K. I. Winey, Y. A. Elabd, J. Runt, and R. H. Colby, Macromolecules **47**, 777 (2014).

9. V. Delhorbe, D. Bresser, H. Mendil-Jakani, P. Rannou, L. Bernard, T. Gutel, S. Lyonnard, and L. Picard, Macromolecules **0**, In press (2017), http://dx.doi.org/10.1021/acs.macromol.7b00197.

0. S. Mogurampelly, J. R. Keith, and V. Ganesan, J. Am. Chem. Soc. **139**, 9511 (2017).

1. W. L. Jorgensen, D. S. Maxwell, and J. Tirado-Rives, J. Am. Chem. Soc. **118**, 11225 (1996).

2. S. V. Sambasivarao and O. Acevedo, Journal of Chemical Theory and Computation **5**, 1038 (2009).

3. M. Frisch, G. Trucks, H. Schlegel, G. Scuseria, M. Robb, J. Cheeseman, G. Scalmani, V. Barone, B. Mennucci, and G. Peterson, *Gaussian 09* (2009).

4. J. M. Wang, R. M. Wolf, J. W. Caldwell, P. a. Kollman, and D. a. Case, J. Comput. Chem. **25**, 1157 (2004).

5. J. Wang, W. Wang, P. A. Kollman, and D. A. Case, Journal of Molecular Graphics and Modelling **25**, 247 (2006).

6. S. Plimpton, Journal of Computational Physics **117**, 1 (1995).

7. L. Martinez, R. Andrade, E. Birgin, and J. Martinez, Journal of computational chemistry **30**, 2157 (2009).

8. R. Hockney and J. Eastwood, *Computer Simulation Using Particles* (CRC Press, 1988), ISBN 9780852743928.

9. S. Plimpton, R. Pollock, and M. J. Stevens, in *Proceedings of the Eighth Siam Conference on Parallel Processing for Scientific Computing* (1997), pp. 1–13.

0. W. Shinoda, M. Shiga, and M. Mikami, Physical Review B - Condensed Matter and Materials Physics **69** (2004).

1. G. J. Martyna, D. J. Tobias, and M. L. Klein, The Journal of Chemical Physics **101**, 4177 (1994).

2. M. Parrinello and A. Rahman, Journal of Applied Physics **52**, 7182 (1981).

3. M. E. Tuckerman, J. Alejandre, R. López-Rendón, A. L. Jochim, and G. J. Martyna, Journal of Physics A: Mathematical and General **39**, 5629 (2006).

4. K. Nakamura, T. Saiwaki, and K. Fukao, Macromolecules **43**, 6092 (2010).

5. K. Nakamura, K. Fukao, and T. Inoue, Macromolecules **45**, 3850 (2012).

6. L. M. Hall, M. E. Seitz, K. I. Winey, K. L. Opper, K. B. Wagener, M. J. Stevens, and A. L. Frischknecht, Journal of the American Chemical Society **134**, 574 (2012).

7. L. M. Hall, M. J. Stevens, and A. L. Frischknecht, Physical Review Letters **106**, 127801 (2011).

8. M. V. O'Reilly, H. Masser, D. R. King, P. C. Painter, R. H. Colby, K. I. Winey, and J. Runt, Polymer (United Kingdom) **59**, 133 (2015).

9. D. S. Bolintineanu, M. J. Stevens, and A. L. Frischknecht, Macromolecules **46**, 5381 (2013).

0. C. F. Buitrago, D. S. Bolintineanu, M. E. Seitz, K. L. Opper, K. B. Wagener, M. J. Stevens, A. L. Frischknecht, and K. I. Winey, Macromolecules **48**, 1210 (2015).

1. H. Liu and S. J. Paddison, ACS Macro Letters **5**, 537 (2016).

2. K. Kimura, J. Motomatsu, and Y. Tominaga, The Journal of Physical Chemistry C **120**, 1238512391 (2016).

3. A. L. Agapov and A. P. Sokolov, Macromolecules **44**, 4410 (2011).

4. J. R. Sangoro, C. Iacob, A. L. Agapov, Y. Wang, S. Berdzinski, H. Rexhausen, V. Strehmel, C. Friedrich, A. P. Sokolov, and F. Kremer, Soft Matter **10**, 3536 (2014).

5. A. Chandra, Physical Review Letters **85**, 768 (2000).

6. W. Zhao, F. Leroy, B. Heggen, S. Zahn, B. Kirchner, S. Balasubramanian, and F. M??ller-Plathe, Journal of the American Chemical Society **131**, 15825 (2009).

7. H. V. R. Annapureddy, H. K. Kashyap, P. M. De Biase, and C. J. Margulis, Journal of Physical Chemistry B **114**, 16838 (2010).